GSA Data Repository Item to accompany: "Probable low-angle thrust earthquakes on the Juan de Fuca/North America plate boundary" by A. M. Trehu, J. Braunmiller, and J.L. Nabelek.

In this supplement, we include additional material to support the results from analysis of regional and teleseismic data that are summarized by Trehu, Braunmiller and Nabelek. We also include tables with the hypocentral parameters of the earthquakes discussed in this paper (Table DR1).

Figure DR1 shows normalized variances for the moment tensor solutions shown in Figure 3 as a function of depth. Table DR2 lists parameters for the shallow-dipping fault plane indicated by the solutions at 6 km depth, which corresponds to the minimum in the normalized residuals for the long-period solution, and the solution at the preferred depth, which has been determined by modeling intermediate and high frequency waveforms, as discussed below. The fault parameters are not very sensitive to depth in this depth range. Figures DR2 and DR3 show the fit of the long period (25-50 s) data to the model for the solution at 6 km. To explore uncertainty in the moment tensor solution for the August 19 event, we also inverted the intermediate period data (5–20s), which show distinct phases that are sensitive to source depth. The intermediate period data suggest that the source was above the Moho at a depth of 17–24 km (Figure DR1 and DR4).

Constraints on the location and depth of the August 19 event were obtained from modeling high frequency observations of the travel time difference between the direct P and the PmP and S arrivals, as discussed in the paper and shown in Figure 4. An additional independent constraint on source depth can be obtained from pP arrivals, which can be observed at a number of quiet stations in central Asia. Examples of these arrivals are shown in Figures DR5 and DR6. The observed time difference between P and pP is 5.0 +- 0.1 s for the July 12 event and 8.0 +- 0.1 s for the August 19 event. Observed travel times were determined by picking the peak to peak time rather than the onset time for each phase; note that P and pP appear to have the same phase for the August 19 event and reversed phase for the July 12 event. These observed times were compared to the travel time calculated for buried sources at several depths. Calculated times are shown for a distance of +-3 km on each side of the source position. For the August 19 event, the model of Figure 4A was used, with the source at km 185. The best fit depth obtained by this method is 15.8 km. For the July 12 event, which was located 38.9 km south of the active source seismic profile in a region where there is strong along-strike variation in the velocity structure of the accretionary complex (see profile 8 in Gerdom et al., 2000). We therefore estimated the depth for the earthquake using 2 different velocity models: (1) at km 160 in the model of Figure 4A and (2) a velocity model with the same depth to the subducted ocean crust as at km 160 but with the overlying velocity derived from the density model for Heceta Bank of Fleming and Trehu (1999). Model 2 is probably a more accurate representation of the velocity structure in the source region for this event, where Miocene-aged sedimentary rocks are exposed at the seafloor. For model 1, the best fit epicentral depth is ~8 km; for model 2 (preferred) it is 11 km, coincident with the interpreted depth of the plate boundary at this position.

Table DR1. Hypocenters for earthquakes since 2003 from the ANSS catalog that fall between 44 and 45°N and 124 and 125°W. All events were reported by the Pacific Northwest Seismic Network. Magnitudes are all coda magnitudes.

Date	Time	Latitude	Longitude	Depth (km)	Magnitude
1/19/03	22:00:32.6	44.455	-124.523	34.0	2.1
10/25/03	02:08:54.9	44.626	-124.411	15.0	2.6
12/7/03	17:37:36.4	44.632	-124.361	24.7	1.2
1/28/04	23:03:42.4	44.641	-124.359	24.0	1.8
2/6/04	06:12:36.1	44.680	-124.327	23.4	2.4
3/21/04	22:35:08.9	44.401	-124.487	22.4	2.2
7/12/04	16:41:18.9	44.342	-124.498	27.9	2.9
7/12/04	16:44:59.8	44.315	-124.566	25.9	4.9
7/13/04	00:26:31.2	44.366	-124.488	28.2	2.7
7/13/04	03:56:11.6	44.359	-124.509	29.4	3.3
7/13/04	15:00:37.2	44.380	-124.508	26.2	2.2
7/14/04	07:44:38.2	44.326	-124.503	0.03	2.3
7/17/04	14:54:55.9	44.343	-124.534	18.2	1.7
7/17/04	16:54:53.8	44.386	-124.497	25.1	1.8
7/19/04	00:14:24.5	44.370	-124.501	26.4	2.8
7/20/04	15:58:48.4	44.338	-124.492	23.7	2.5
7/27/04	23:28:26.7	44.345	-124.481	25.4	2.3
8/19/04	06:06:03.6	44.664	-124.300	27.9	4.7
8/19/04	06:26:00.5	44.646	-124.346	24.6	2
8/19/04	07:54:10.9	44.651	-124.340	24.9	2.5
8/23/04	08:04:44.6	44.668	-124.344	23.6	2.3
4/13/05	04:51:05.9	44.422	-124.333	28.9	2.5
4/23/05	01:38:02.5	44.447	-124.644	28.0	1.4
6/1/05	07:20:00.3	44.333	-124.484	26.7	1.8
8/13/05	17:41:13.0	44.413	-124.428	28.0	2.2
9/26/05	18:11:05.0	44.322	-124.590	33.3	2.1
4/8/07	09:34:32.4	44.330	-124.620	40.2	1.8
5/17/07	09:35:09.7	44.381	-124.489	28.1	1.7
8/23/07	22:31:00.1	44.629	-124.331	27.3	2.8
8/24/07	03:30:24.1	44.639	-124.326	28.6	1.3
8/24/07	12:22:39.4	44.625	-124.326	27.0	1.1
8/25/07	01:09:41.3	44.371	-124.396	34.1	1.3

Table DR2. Results from the moment tensor analysis for the two mainshocks from analysis of 25-50 s data. We show the result for the depth giving the smallest varience and for the depth that best fits the PmP and/or pP travel time analysis. The azimuth is the horizontal projection of the slip vector.

Event	Depth	Strike	Dip	Rake	Moment ($x10^{16}$Nm)	Mw	Azimuth
07/12/04	6	353	16	75	2.7	4.9	99
07/12/04	12	356	25	82	2.4	4.9	95
08/19/04	6	349	7	99	2.0	4.8	70
08/19/04	15	322	13	70	1.5	4.7	72

Figure DR1. Normalized variance of solutions as a function of source depth for the long period (solid lines) and intermediate period (dashed line) solutions. Only the 8 closest stations (distance 30–220 km) were used for the intermediate period inversions. The overall higher variance of the intermediate solution is due to inclusion of shorter period data. We have not yet identified why our routine long-period analysis of the August 19 earthquake was anomalously insensitive to source depth. The dip of the fault plane and the azimuth of the slip vector are not sensitive to source depth, to the velocity model, or to the subset of stations selected for inversion. The long-period inversions were done assuming a simple one-dimensional velocity model (Fig. DR7). The intermediate period inversions were done with a one-dimensional velocity model extracted from the model of Figure 4A at km 225 (Fig. DR7).

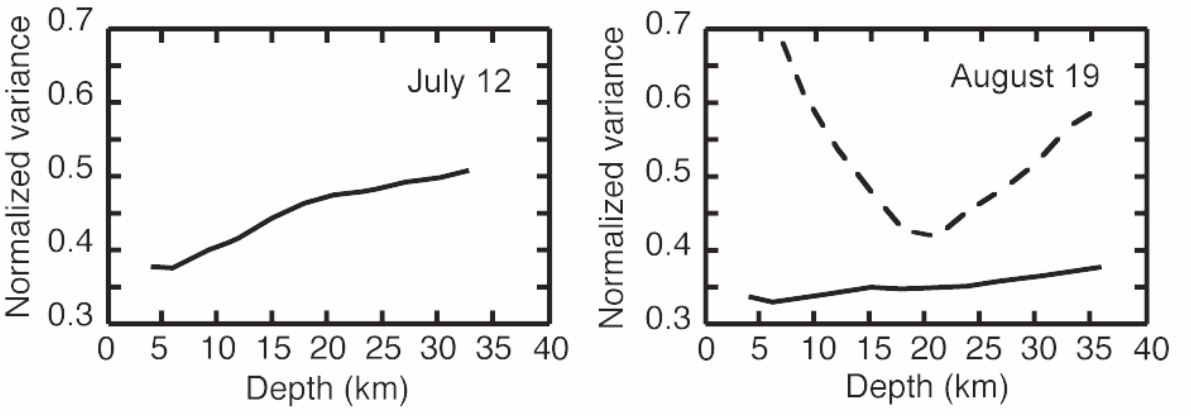

Figure DR2. Observed (solid black) and synthetic (dashed red) seismograms for the best fit model (6 km depth) in the 25-50 s period band for the July 12, 2004 earthquake. Z, R, and T are vertical, radial, and transverse components. All seismogram amplitudes are normalized to 100 km epicenter distance assuming cylindrical spreading. Stations are listed in azimuthal order with numbers beneath codes giving event-station azimuth and distance. Triangles on fault plane solution show station coverage.

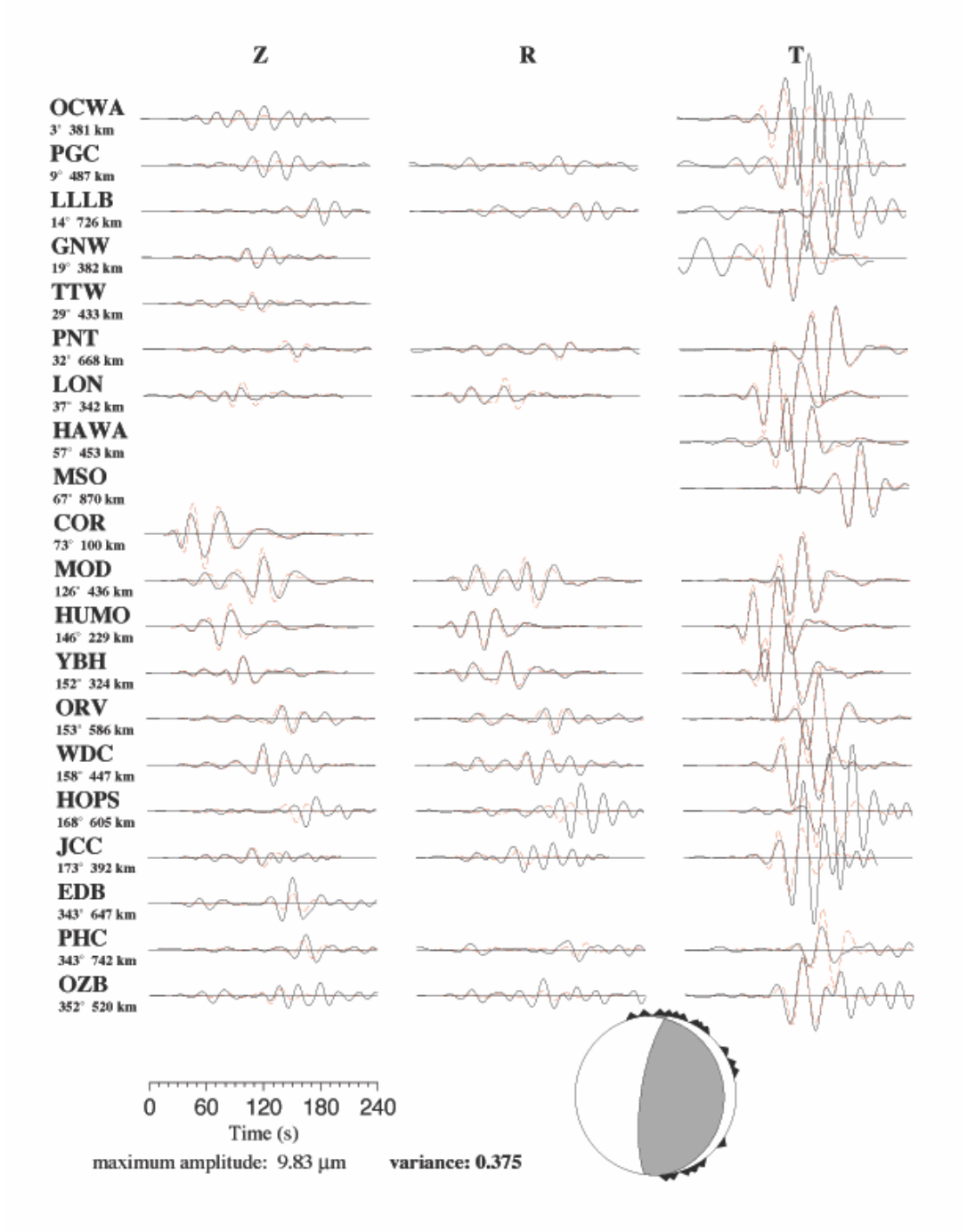

Figure DR3. Observed (solid black) and synthetic (dashed red) seismograms for the best fit model (6 km depth) in the 25-50 s period band for the August 19, 2004 earthquake. Z, R, and T are vertical, radial, and transverse components. All seismogram amplitudes are normalized to 100 km epicenter distance assuming cylindrical spreading. Stations are listed in azimuthal order with numbers beneath codes giving event-station azimuth and distance. Triangles on fault plane solution show station coverage.

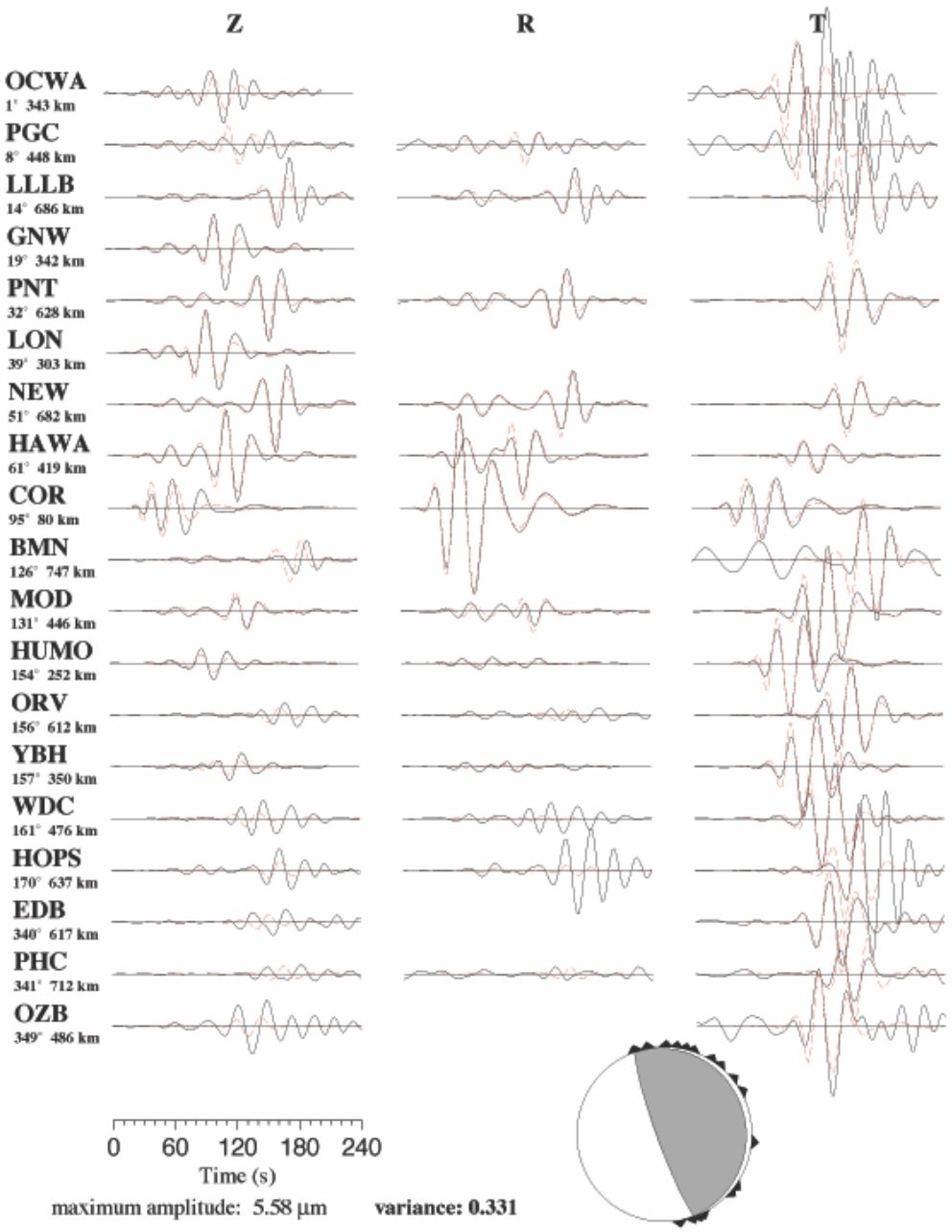

Figure DR4. Depth resolution from 5-20 s period band waveform inversion using stations within 220 km of the source. Observed (solid black) and synthetic (dashed red) seismograms for station COR are shown for several source depths (indicated by numbers on the left). Depth is constrained primarily by the Z component and indicates a source depth that is greater than the depth obtained from long-period data (Figure DR3).

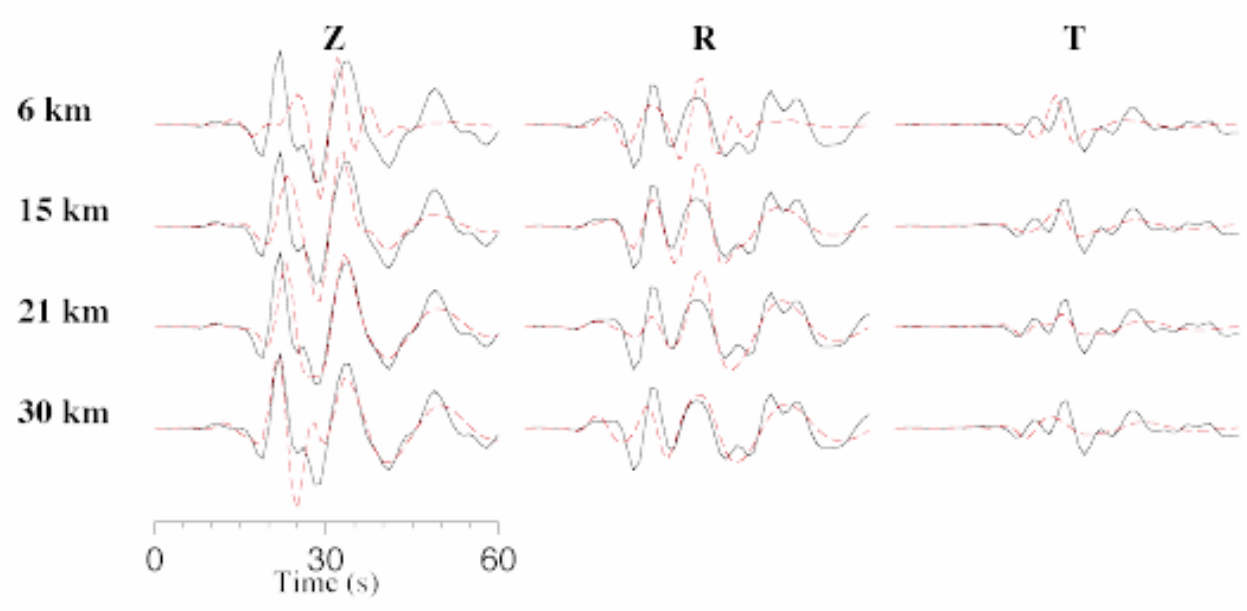

Figure DR5. Seismograms from stations BRVK (Borovke) and KURK (Kirkuk) showing P and pP arrivals for the August 19, 2004, earthquake. Graph on the right shows the travel time to the surface from sources at different depths located at a distance of 185 km along the model. This time should be ~0.5 times the time difference between P and pP (8.0 s).

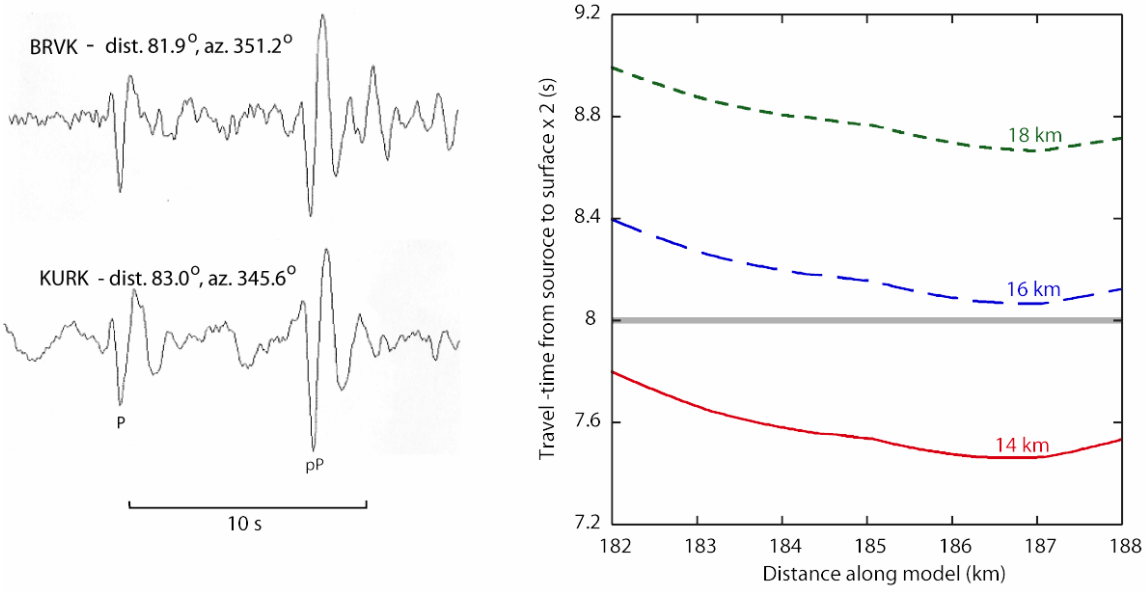

Figure DR6. Seismograms from stations BRVK (Borovke) and KURK (Kirkuk) showing P and pP arrivals for the July 12, 2004, earthquake. Graph on the right shows the travel time to the surface from sources at 7 and 9 km depth located at a distance of 160 km along the model and for 11 and 9 km depth for a model with the same depth to the plate boundary but with water depth and crustal velocity corresponding to Heceta Bank. This time should be ~0.5 times the time difference between P and pP (5.0 s).

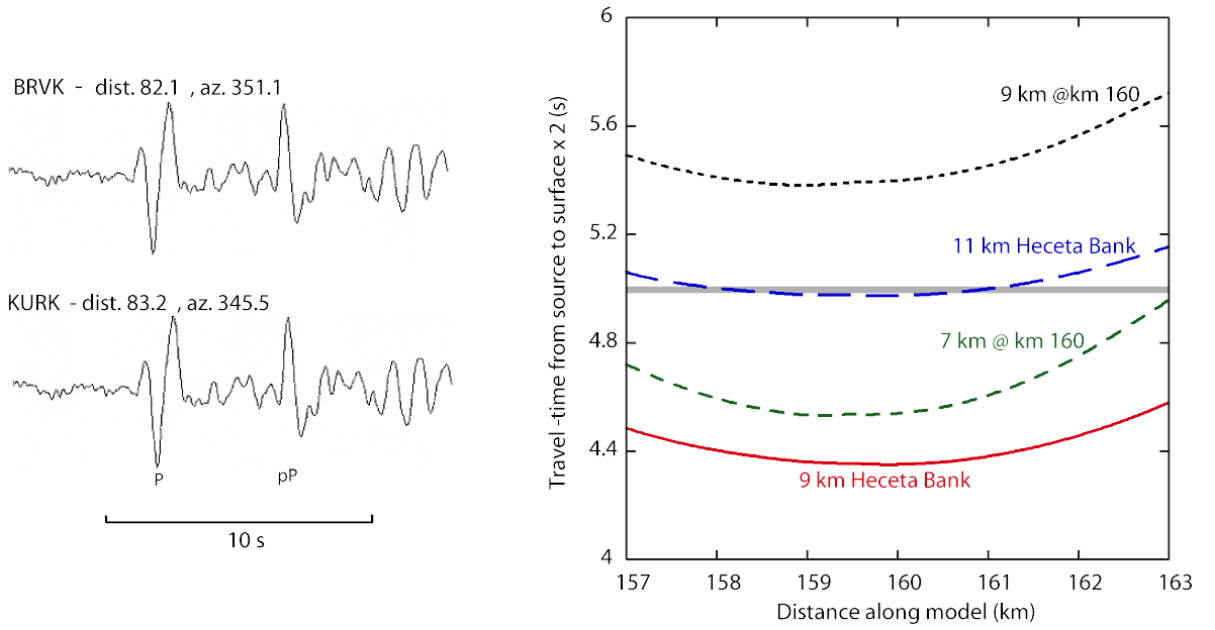

Figure DR7. Velocity models used for Figures D1-D6.